SCIENCE CHINA
Information Sciences

April 2019, Vol. 62 040304:1–040304:3
https://doi.org/10.1007/s11432-018-9744-2

• LETTER •
Special Focus on High-Resolution Radar

Improved track-before-detect method for detecting range-spread targets in generalized Pareto clutter

Jian XUE[1], Shuwen XU[1,2*] & Penglang SHUI[1]

[1]*National Lab of Radar Signal Processing, Collaborative Innovation Center of Information Sensing and Understanding, Xidian University, Xi'an* 710071*, China;*
[2]*Department of Electrical and Computer Engineering, Mcmaster University, Hamilton* L8S 4K1*, Canada*

Received 3 July 2018/Revised 8 September 2018/Accepted 6 December 2018/Published online 20 February 2019

Citation Xue J, Xu S W, Shui P L. Improved track-before-detect method for detecting range-spread targets in generalized Pareto clutter. Sci China Inf Sci, 2019, 62(4): 040304, https://doi.org/10.1007/s11432-018-9744-2

Dear editor,
High-resolution radars demonstrate a good target-detection performance, especially for weak targets such as periscopes and small boats [1]. Methods for adaptive detection employed by high-resolution maritime radars usually consider range-spread targets and non-Gaussian sea-clutter. In this case, the energy of a range-spread target at each occupied cell should be integrated along the range dimension. On the other hand, non-Gaussian sea clutter may contain discrete sea spikes that look similar to the targets. Due to their long duration and high power, sea spikes can cause a high probability of false alarms (PFA). Therefore, the impact of non-Gaussian clutter including sea spikes should be minimized when developing methods for weak range-spread target detection.

The generalized Pareto distribution with inverse Gamma texture has been shown to be suitable for heavy-tail clutter; hence, it has been exploited to describe non-Gaussian clutter [2]. An optimal coherent detector for range-spread targets has been developed in generalized Pareto clutter with inverse Gamma texture [3]. Traditional coherent detectors are used to detect targets with several pulses and high signal-to-clutter ratios. However, they suffer significant performance losses when detecting weak targets. Long-time integration is an effective way to improve the detection performance. Therefore, multi-scan radar returns are typically used to detect weak targets instead of detecting them in a single scan. The dynamic-programming-based track-before-detect (DP-TBD) technique [4] is a practical method for detecting weak targets. Range-spread target detection based on DP-TBD has been investigated in compound-Gaussian clutter with an unknown texture distribution [5].

For the range-spread target detection, the number of occupied range cells is usually assumed to be known; however, it cannot be known in practical applications. At the same time, weak range-spread targets may not be effectively detected during a single scan period. Consequently, we focus on the problem of adaptively detecting weak range-spread targets embedded in non-Gaussian sea clutter that may include sea spikes.

Detection problem description. The considered surveillance area is divided into $N_r \times N_\theta$ grid cells, where N_r and N_θ are the number of cells at the range and azimuth, respectively. K consecutive scanning returns are processed to detect a range-spread target. The number of coherent pulses in a coherent processing interval is N. The decision on the existence of a moving target embedded in a clutter-dominated region can be formulated in

---

[*] Corresponding author (email: swxu@mail.xidian.edu.cn)

terms of the following binary hypothesis testing:

$$\begin{cases} \mathrm{H}_0: \boldsymbol{z}_k^{r,\theta} = \boldsymbol{c}_k^{r,\theta}, r \in [1, N_r], \\ \theta \in [1, N_\theta], k \in [1, K], \\ \mathrm{H}_1: \begin{cases} \boldsymbol{z}_k^{r,\theta} = \alpha_k^{r,\theta}\boldsymbol{p} + \boldsymbol{c}_k^{r,\theta}, & r \in \Theta, \theta = \theta_k, \\ \boldsymbol{z}_k^{r,\theta} = \boldsymbol{c}_k^{r,\theta}, & \text{else}, \end{cases} \end{cases} \tag{1}$$

where H_0 denotes clutter-only, H_1 means that a range-spread target appears in $\Theta = \{r_k + 1, r_k + 2, \ldots, r_k + L\}$ of the θ_kth azimuth and other positions contain clutter-only, L is the number of range cells occupied by the target, $\boldsymbol{c}_k^{r,\theta}$ is the N-dimensional clutter vector at the rth range cell of the θth azimuth, $\alpha_k^{r,\theta}$ is the unknown deterministic target complex amplitude, and $\boldsymbol{p}$ is the normalized steering vector. The target state at the kth scan can be expressed as $\boldsymbol{s}_k = [r_k, \dot{v}_{r,k}, \theta_k, \dot{v}_{\theta,k}]^{\mathrm{T}}$, where r_k and θ_k are the range and azimuth position at the kth scan, $\dot{v}_{r,k}$ and $\dot{v}_{\theta,k}$ denote the target velocities at the range and azimuth dimensions, respectively, and $(\cdot)^{\mathrm{T}}$ denotes a transposition.

In a coherent processing interval, the clutter vector $\boldsymbol{c}_k^{r,\theta}$ can be described as

$$\boldsymbol{c}_k^{r,\theta} = \sqrt{\tau_k^{r,\theta}}\boldsymbol{u}_k^{r,\theta}, \tag{2}$$

where the speckle $\boldsymbol{u}_k^{r,\theta}$ is a complex Gaussian vector with zero mean and the covariance matrix $\boldsymbol{R}_k^{r,\theta}$; the texture $\tau_k^{r,\theta}$ obeys the inverse Gamma distribution:

$$f(\tau_k^{r,\theta}) = \frac{1}{\Gamma(\lambda)\mu^\lambda}(\tau_k^{r,\theta})^{-(\lambda+1)}\mathrm{e}^{\frac{-1}{\mu\tau_k^{r,\theta}}}, \tag{3}$$

where $\Gamma(\cdot)$ denotes the Gamma function, μ is the scale parameter and λ is the shape parameter.

Detection method design. Non-coherent integration along the occupied range cells is performed to detect a range-spread target after coherent integration along the pulse dimension. For coherent integration of the pulse dimension at the kth scan, the optimal adaptive detector can be expressed as

$$\frac{\left|(\boldsymbol{p}_k^{r,\theta})^{\mathrm{H}}(\hat{\boldsymbol{R}}_k^{r,\theta})^{-1}\boldsymbol{z}_k^{r,\theta}\right|^2}{q_0\left[(\boldsymbol{p}_k^{r,\theta})^{\mathrm{H}}(\hat{\boldsymbol{R}}_k^{r,\theta})^{-1}\boldsymbol{p}_k^{r,\theta}\right]} \underset{\mathrm{H}_0}{\overset{\mathrm{H}_1}{\gtrless}} \eta, \tag{4}$$

where $q_0 = [1/\mu + (\boldsymbol{z}_k^{r,\theta})^{\mathrm{H}}(\hat{\boldsymbol{R}}_k^{r,\theta})^{-1}\boldsymbol{z}_k^{r,\theta}]$, $\hat{\boldsymbol{R}}_k^{r,\theta}$ is the estimated covariance matrix and η is the detection threshold. A high PFA threshold is used to make the majority of the clutter test statistics being blocked and the target signal being preserved to reduce the computational complexity of the subsequent DP-TBD operation and solve the case when the number of range cells occupied by the target is unknown.

After the threshold processing, the remaining test statistics of the target and high-power sea clutter are used in non-coherent integration performed by the improved DP-TBD method. The target echo is continuous in several range cells, while the high-power sea clutter is random and discrete. Consequently, we consider the continuous non-zero-value cells as a unitary target state to solve the problem of the unknown number L of range cells. This operation enables maximum integration of the range-spread target along the range dimension while reducing the computational complexity of DP-TDB as a result of the decreased number of the target states. For the target states $\boldsymbol{s}_K = [r_K, \dot{v}_{r,K}, \theta_K, \dot{v}_{\theta,K}]^{\mathrm{T}}$, s.t. $\xi_K^{r,\theta} > 0$, $1 \leqslant r \leqslant N_s < N_r$, $1 \leqslant \theta \leqslant N_\theta$, $\dot{v}_{r,K}$ and $\dot{v}_{\theta,K} \in [-V_{\max}, V_{\max}]$, the merit function of $\boldsymbol{s}_K$ is $I_K(\boldsymbol{s}_K) = \xi_K^{r,\theta}$, where N_s denotes the number of target states and $V_{\max}$ is the maximum velocity of the moving target. Then the DP recursion is implemented. When $2 \leqslant k \leqslant K$, the merit function $I_k(\boldsymbol{s}_k) = \max_{\boldsymbol{s}_{k-1}\in\psi(\boldsymbol{s}_{k-1})}[I_{k-1}(\boldsymbol{s}_{k-1})] + \xi_k^{r,\theta}$, where $\psi(\boldsymbol{s}_{k-1})$ is a collection of target states at $(k-1)$th scan and $\xi_k^{x,y} > 0$. The threshold processing may result in the target state collection to be $\psi(\boldsymbol{s}_k) = 0$, $k \in [1, \ldots, K-1]$. In this case, we use the original test statistics of these zero target states and consider the maximum test statistic and its position as the most probable target state.

The abovementioned operation may result in a high number of sea spikes being integrated between radar scans; hence, we modify the merit function as follows:

$$\tilde{I}_K(\boldsymbol{s}_K) = \alpha \cdot I_K(\boldsymbol{s}_K), \tag{5}$$

where $\tilde{I}_K(\boldsymbol{s}_K)$ denotes the final merit function, the mark parameter $\alpha = \varepsilon(K - N_0 - N_g), 0 \leqslant N_0 \leqslant K - 1$, $\varepsilon(\cdot)$ is the step function, N_0 denotes the time when all transferred target states of a target state at all K scans are zero, N_g denotes a threshold to judge whether the target state at Kth scan is a sea spike or not. If the number of times when a target state is non-zero at all K scans is less than N_g, then, we consider that the target state is a sea spike. Finally, a detection threshold for multi-scan integration is used to detect targets.

Performance assessment. The results of evaluating the detection performance of the improved DP-TBD method are depicted in Figure 1. Simulated generalized Pareto clutter with different shape parameters is used to verify the performance of the improved DP-TBD and GLRT-DP-TBD [5] methods, as illustrated in Figure 1(a). The experiment parameters are $K = 5$, $N = 8$, $N_r = 20$, $N_\theta = 1$, $\dot{v}_{r,k} = 1$, $\dot{v}_{\theta,k} = 0$, $\eta_k^{r,\theta} = 0$, $L = 4$,

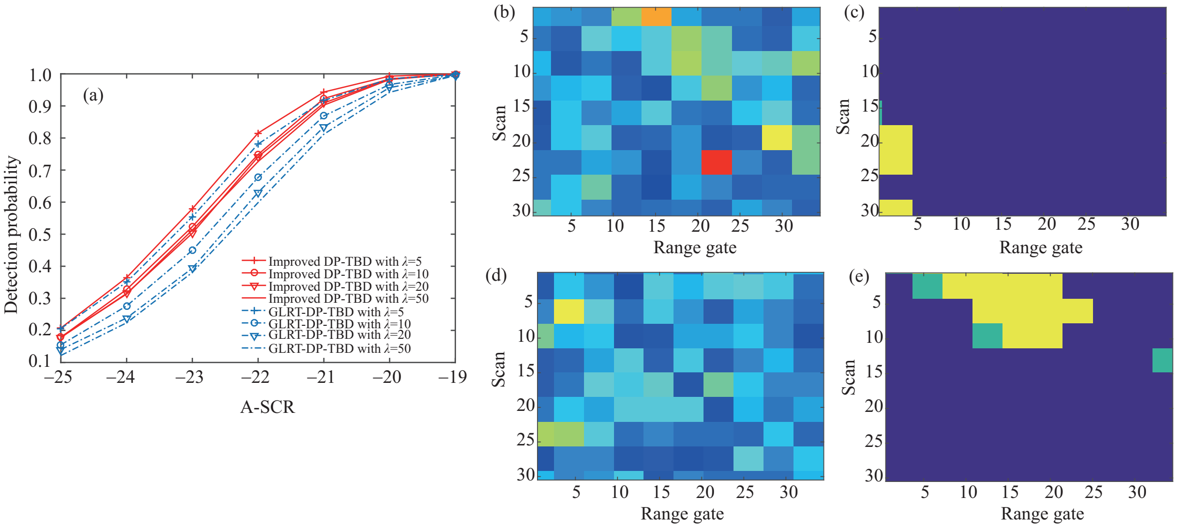

Figure 1 (Color online) Performance evaluation. (a) Performance curves; (b) power map of the returns with A-SCR = 2 dB; (c) detection (yellow) and missed (green) results with A-SCR = 2 dB; (d) power map of the return with A-SCR = 6 dB; (e) detection (yellow) and missed (green) results with A-SCR = 6 dB.

the target Doppler frequency is $f_d = 0.3$, $\mu = 1$, and $P_{\mathrm{fa}} = 10^{-3}$. It can be seen from Figure 1(a) that the improved DP-TBD method outperforms GLRT-DP-TBD. In Figures 1(b)–(e), the detection results of the improved DP-TBD method are shown based on the measured IPIX sea-clutter data [6]. A simulated weak range-spread target with uniform motion is added to the measured sea clutter. The data contain 30 scans with $N_r = 34$ and $N = 8$. Other parameters are set as $K = 5$, $N_\theta = 1$, $\dot{v}_{r,k} = 1$, $\dot{v}_{\theta,k} = 0$, $L = 4$, and $f_d = 0.3$. For simplicity, prior information about the velocity is assumed to be known. The data from all 30 scans is processed using the improved DP-TBD method in a way of slide windows [7]. In practical applications, the number L of range cells occupied by a range-spread target may vary across radar scans due to the target motion. Thus, L is considered to randomly vary within the set of {1, 2, 3, 4, 5}. Figures 1(b) and (d) depict the power of the simulated target in addition to that of the measured sea clutter. It can be seen that the number of range cells occupied by the target fluctuates across the scans. Figures 1(c) and (e) present the detection and missed results with yellow and green colors, respectively. As can be observed from Figures 1(c) and (e), the proposed method can efficiently detect the range-spread target when L is unknown and varies across scans.

Conclusion. We proposed an improved DP-TBP method for detecting weak range-spread targets with an unknown number of occupied range cells in non-Gaussian clutter, including sea spikes. The experimental results showed that the improved DP-TBD method performs better than GLRT-DP-TBD and achieves satisfactory detection results. Our next plan is to further investigate the performance of the improved DP-TBD method in practical applications.

Acknowledgements This work was supported by National Natural Science Foundation of China (Grant No. 61871303), Natural Science Basic Research Plan in Shaanxi Province of China (Grant No. 2017JM6031), Young Talent fund of University Association for Science and Technology in Shaanxi (Grant No. 20160205), CSC visiting scholar foundation (Grant No. 201706965034), and Foreign Scholars in University Research and Teaching Programs (the 111 Project) (Grant No. B18039).

References

1 Carretero-Moya J, Gismero-Menoyo J, Blanco-del-Campo A, et al. Statistical analysis of a high-resolution sea-clutter database. IEEE Trans Geosci Remote Sens, 2010, 48: 2024–2037
2 Sangston K J, Gini F, Greco M S. Coherent radar target detection in heavy-tailed compound-gaussian clutter. IEEE Trans Aerosp Electron Syst, 2012, 48: 64–77
3 Shang X Q, Song H J, Wang Y, et al. Adaptive detection of distributed targets in compound-Gaussian clutter with inverse gamma texture. Digit Signal Process, 2012, 22: 1024–1030
4 Yi W, Jiang H C, Kirubarajan T, et al. Track-before-detect strategies for radar detection in G0-distributed clutter. IEEE Trans Aerosp Electron Syst, 2017, 53: 2516–2533
5 Jiang H C, Yi W, Cui G L, et al. Track-before-detect strategies for range distributed target detection in compound-Gaussian clutter. Signal Process, 2016, 120: 462–467
6 Currie B, Bakker R. The McMaster IPIX radar sea clutter database. http://soma.ece.mcmaster.ca/ipix/
7 Yi W, Kong L J, Yang J Y. Thresholding process based dynamic programming track-before-detect algorithm. IEICE Trans Commun, 2013, 96: 291–300